

# Emission Lines as a Tool in Search for Supermassive Black Hole Binaries and Recoiling Black Holes

Tamara Bogdanović

*Department of Astronomy, University of Maryland, College Park, MD 20742*

Michael Eracleous, Steinn Sigurdsson

*Department of Astronomy & Astrophysics and Center for Gravitational Wave Physics, Pennsylvania State University, State College, PA 16802*

arXiv:0909.0516v1 [astro-ph.CO] 2 Sep 2009

---

## Abstract

Detection of electromagnetic (EM) counterparts of pre-coalescence binaries has very important implications for our understanding of the evolution of these systems as well as the associated accretion physics. In addition, a combination of EM and gravitational wave signatures observed from coalescing supermassive black hole binaries (SBHBs) would provide independent measurements of redshift and luminosity distance, thus allowing for high precision cosmological measurements. However, a statistically significant sample of these objects is yet to be attained and finding them observationally has proven to be a difficult task. Here we discuss existing observational evidence and how further advancements in the theoretical understanding of observational signatures of SBHBs before and after the coalescence can help in future searches.

*Key words:* Supermassive black hole binaries, recoiling supermassive black holes, observational signatures, emission line profiles, optical light curves, X-ray light curves, radiative transfer, hydrodynamics

*PACS:* 04.70.-s, 47.70.Mc, 95.30.Lz, 98.54.Aj, 98.62.Mw

---

## 1. Introduction

The most direct evidence for the formation of supermassive black hole binaries (SBHBs) currently available through electromagnetic (EM) observations is the existence of black hole pairs spatially resolved on the sky. An example of such a system is NGC 6240, an ultra-luminous infrared galaxy in which the *Chandra* X-ray observatory revealed a merging pair of X-ray emitting active nuclei with a separation of  $\sim 1$  kpc (Komossa et al., 2003). The large observed separation implies that the two supermassive black holes (SBHs) are a pair of unrelated massive objects orbiting in the potential of the host galaxy that are yet to reach the binary stage, in which the two SBHs will be bound by their mutual gravitational force. Practical obstacles in the direct identification of close binaries via EM observations arise from the need for a very high spatial resolution and accuracy in position measurements. Because of the small orbital separation of sub-parsec binaries and the small separation of recoiling SBHBs from the centers of their host galaxies not too long after the coalescence<sup>1</sup>, the best prospect for *direct imaging* of these objects is offered by radio interferometers, provided that SBHBs and recoiling SBHBs are radio sources. Since this method relies on pointed observations of candidate objects, it requires *a priori* knowledge about their

location on the sky. This technique yielded one binary candidate, 0402+379, an object with two compact, unresolved radio-cores at a projected separation of only  $\sim 7$  pc, observed with the *Very Long Baseline Array* (VLBA; Maness et al., 2004; Rodriguez et al., 2006). Followup multi-wavelength observations of this and similar radio candidates in the future are essential for studying the rest of associated observational signatures.

The second most compelling piece of observational evidence for a SBHB is a periodic signal associated with Keplerian motion, such as the periodic or quasi-periodic variability of the light emitted by an object. A binary candidate selected according to this criterion is the blazar OJ 287, which exhibits outburst activity in its optical light curve with a period close to 12 years (Valtonen et al., 2008). Distinguishing periodic variability due to a binary from the common variability of active galactic nuclei (AGNs) can be challenging because it relies on long-term monitoring of the candidates and is, in many cases, less pronounced than in OJ 287.

The third technique used to select SBHB candidates relies on a *detection of the Doppler-shift* in the spectrum of an object that arises from the orbital motion of a binary. In this case the search utilizes the emission-lines associated with multiple velocity systems in the spectrum of a candidate object. Because this effect is also expected to arise in case of a recoiling SBHB receding from its host galaxy, the same approach is used to “flag” candidates of that type. The Doppler shift signature is however not unique to these two physical scenarios, and complementary observations are needed in order to determine the true

---

*Email address:* tamarab@astro.umd.edu (Tamara Bogdanović)

<sup>1</sup>SBH recoil considered here is due to postulated asymmetric gravitational wave emission, as shown by numerical relativity.

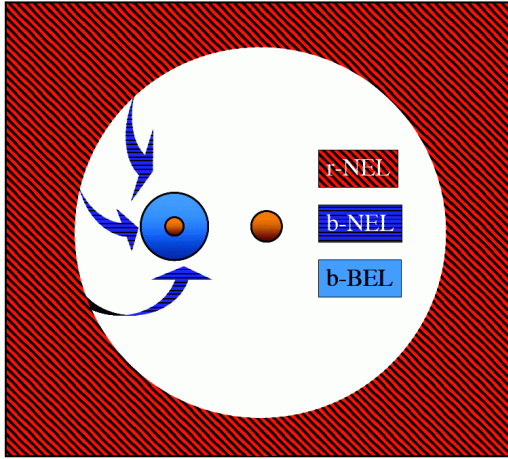


Figure 1: Illustration of the binary model for J0927. The innermost region of a circumbinary disk is shown after the binary has cleared a low density “hole” in the disk (top view, not drawn to scale). In this model r-NELs are associated with the circumbinary disk, b-BELs with the disk surrounding the less massive secondary SBH, and b-NELs with the accretion streams flowing from the inner edge of the circumbinary disk toward the secondary. Figure adapted from Bogdanović et al. (2009).

nature of observed candidates (as discussed in §1.1). The advantage of the method is its simplicity, as emission spectra that exhibit Doppler shift signatures are relatively straightforward to select from large archival data sets, such as the Sloan Digital Sky Survey (SDSS). So far a few SBHB candidates have been selected out of  $\sim 21,000$  SDSS quasars: J092712.65+294344.0 (hereafter J0927; Bogdanović et al., 2009; Dotti et al., 2009), J153636.22+044127.0 (J1536; Boroson & Lauer, 2009), and J105041.35+345631.3 (J1050; Shields et al., 2009b), where the first and the last object have also been flagged as recoiling SBH candidates (Komossa et al., 2008; Shields et al., 2009b). In the following section we describe in more detail results and uncertainties associated with this approach, using J0927 as an illustrative example, and summarize the status of the other two candidates.

### 1.1. SBHB candidates: J0927, J1536, and J1050

The optical spectrum of J0927 features two sets of emission lines offset by  $2650 \text{ km s}^{-1}$  with respect to each other. The “redward” system consists of only narrow emission lines (r-NELs), while the “blueward” emission-line system comprises broad Balmer lines (b-BEL) and narrow, high-ionization forbidden lines (b-NELs). In the context of the binary model, the observed velocity shift represents the projected orbital velocity of the less massive member of a bound black hole pair. In this model, the emission lines of the blueward system (b-NELs and b-BELs) originate in gas associated with the less massive, secondary black hole, while the r-NELs originate in the interstellar matter (ISM) of the host galaxy. An illustration of the proposed geometry for the binary model is shown in Figure 1. For an assumed inclination and orbital phase angles of  $45^\circ$  and a mass ratio of  $q = 0.1$ , the inferred orbital period and mass of the binary are  $\sim 190 \text{ yr}$  and  $\sim 10^9 M_\odot$ , respectively. The accreting secondary is the main source of ionizing radiation while

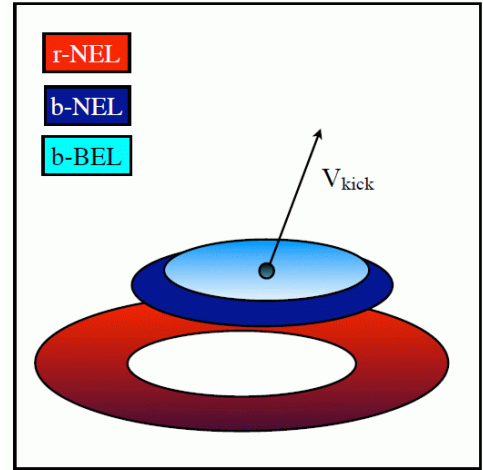


Figure 2: Illustration of the model of a recoiling SBH proposed for J0927 by Komossa et al. (2008) (oblique view, not drawn to scale). In this model r-NELs are associated with the ISM of the host galaxy, b-BELs with the disk recoiling with the SBH, and b-NELs with the expanding accretion disk, swept up ISM, or associated outflows.

the primary is either quiescent or much fainter.

According to the recoiling SBH interpretation for J0927 (note that this was the first explanation proposed for this object by Komossa et al., 2008), the b-BELs originate in the broad-line region retained by the SBH, the b-NELs were attributed to gas that is marginally bound to the SBH, swept up or outflowing, and the r-NELs are associated with the ISM of the host galaxy (the geometry of the recoiling SBH model is outlined in Figure 2). In this model the recoiling SBH of mass  $\sim 6 \times 10^8 M_\odot$  appears as an AGN during the period in which it accretes from the disk that is carried along with the hole. The accreting SBH provides a source of ionizing radiation for the b-BELs and b-NELs, as well as for the r-NELs, albeit from a larger distance.

Another class of proposed explanations for J0927 includes interaction of two galaxies in the potential well of a massive cluster (Heckman et al., 2009) and a superposition of otherwise unrelated AGN in a cluster environment (Shields et al., 2009a). Both of these scenarios can, in principle, explain the multiple velocity-emission-line systems seen in the spectrum of J0927 and offer a good alternative to the SBHB and recoiling SBH models. In a subsequent paper, however, Decarli et al. (2009a) reported that J0927 is unlikely to be a member of a rich cluster. At this point every model proposed for J0927 received some amount of criticism (see the above papers for details) and thus, the nature of J0927 is not conclusively determined and requires further investigation.

Soon after its discovery, the interpretation for the candidate J1536 was called into question because of the lack of the variability expected from Keplerian motion (Chornock et al., 2009a; Gaskell, 2009) and the similarity of its line profiles to those of “double-peaked emitters” (Chornock et al., 2009b). At this point, the data available for this object do not conclusively rule out the binary scenario and further observational tests have been suggested (Wrobel & Laor, 2009; Lauer & Boroson, 2009; Decarli et al., 2009b).

Most recently, Shields et al. (2009b) reported the discovery of another unusual SDSS quasar, J1050, for which an SBHB is a viable explanation, along with a recoiling SBH, and a double-peaked emitter. As with the previous cases, further observations are needed in order to discriminate among proposed hypotheses.

J0927, J1536, and J1050 do not make up a uniform class of objects because their emission-line spectra differ from each other. A common property shared by all three objects is that their emission line systems exhibit shifts in the range  $2000 - 4000 \text{ km s}^{-1}$ . If such velocity shifts are interpreted in the context of a binary model, and if the emission-line systems are associated with one or both of the black holes, the expectation is that the orbital motion of the binary should give rise to a measurable velocity change of the emission lines on a time-scale of several years. For all three objects this basic test was carried out by taking spectra of the object at a few different epochs and measuring the change in the position of the emission line peaks. In all three cases the measured rate of velocity shift is very low ( $dv/dt \sim \text{few} \times 10 \text{ km s}^{-1} \text{ yr}^{-1}$ ) and consistent with zero within the error bars. Taken at the face value this result seems to eliminate the possibility that any of the three candidate objects is a binary. However, it may also be that if the selection process is biased towards binaries with large velocity shifts, they may be easiest to spot precisely when they are close to quadrature and  $dv/dt$  is small. Hence, it may take longer to detect a change in  $dv$  than expected if time scale is estimated based on a random phase prior. Moreover, the uncertainties in emission geometry and radiative processes of binary accretion flows currently preclude elimination of the binary model based on the lack of velocity shifts measured from the line peaks (see discussion in §3.1).

In the following section we briefly describe theoretical ideas for formation and evolution of SBHBs, including the consequences of their coalescence.

## 2. Astrophysics of SBHBs before and after coalescence

Galactic mergers are expected to be the major route for formation of binary black holes, in agreement with predictions of hierarchical models of structure formation (Haehnelt & Kauffmann, 2002; Volonteri et al., 2003) and the observation that the majority of galaxies harbor massive black holes in their centers (e.g., Kormendy & Richstone, 1995; Richstone et al., 1998; Peterson & Wandel, 2000; Ferrarese & Ford, 2005). Following a galactic merger, the two SBHs are initially carried within their host bulges and eventually find themselves at  $\sim \text{kpc}$  separations (e.g., Kazantzidis et al., 2005) from each other. In this first evolutionary stage, the separation of a pair of the SBHs decreases through the process of dynamical friction that involves two-body gravitational interaction of individual SBHs with stars and interactions with gas in the nuclear region. In the second stage (at separations  $\lesssim 10 \text{ pc}$ ), the binary becomes gravitationally bound when the binary mass exceeds that of the gas and stars enclosed within its orbit. The evolution of the binary in this phase is determined by the availability of stars

for three-body interactions (Berczik et al., 2006; Sesana et al., 2007a; Perets et al., 2007) and the availability of gas which can transport the excess angular momentum of the binary (Begelman et al., 1980; Ivanov et al., 1999; Gould & Rix, 2000; Armitage & Natarajan, 2002; Escala et al., 2004, 2005; Dotti et al., 2006, 2007; Mayer et al., 2007; Colpi et al., 2007; Cuadra et al., 2009; Hayasaki, 2009). In the third and final stage (at separations  $< 10^{-2} \text{ pc}$ ), the binary is led to coalesce by the emission of gravitational waves (GWs) and forms a single, remnant SBH with mass slightly lower (typically by several percent) than that of the two parent SBHs combined. Due to asymmetries in the orientation of the black hole spin axes with respect to the binary orbital axis, and the masses of the two SBHs with respect to each other, the emission of GWs is, in general, not isotropic. The GWs carry net linear momentum in some direction, causing the center of mass of the binary to recoil in the opposite direction.

If the candidates described in §1.1 turn out to be SBHBs, these would most likely correspond to binaries in the second evolutionary stage. Several physical processes may contribute to the presence of a, hopefully unique, spectral signature of such binaries: the presence of one or two (unresolved) accretion disks *around individual black holes*, albeit in general of different luminosity; the tidal distortion of the inner parts of the *circumbinary* disk by the presence of the binary (similar to features seen in proto-planetary disks).

The “mass loss” and gravitational rocket effect at the end of the third evolutionary stage of the binary can have profound effects on the surrounding gas and potentially give rise to unique observational signatures as was recently suggested by a number of authors (Loeb, 2007; Shields & Bonning, 2008; Lippai et al., 2008; Schnittman & Krolik, 2008; Kocsis & Loeb, 2008; Mohayaee et al., 2008; Devecchi et al., 2009; O’Neill et al., 2009). Namely, the results of numerical relativity calculations show that recoil velocity of a remnant SBHs can range from about  $200 \text{ km s}^{-1}$  for SBHs with low spins or spin axes aligned with the orbital axis (Herrmann et al., 2007a,b; Baker et al., 2006, 2007; González et al., 2007) to a remarkable  $\sim 4000 \text{ km s}^{-1}$  in case of maximally spinning SBHs with spins oppositely directed and in the orbital plane (Campanelli et al., 2007a,b). If following a galactic merger the two SBHs find themselves in a gas rich environment, gas accretion torques will act to align their spin axes with the orbital axis, thus reducing the maximum kick to a value well below the galactic escape speed (the escape speed from most galaxies is  $< 2000 \text{ km s}^{-1}$ , Merritt et al., 2004). This effect is expected to increase the chance of retention of recoiling SBHs by their host galaxies (Bogdanović et al., 2007), in agreement with the observation that almost all galaxies with bulges appear to have a central SBH (Ferrarese & Ford, 2005). However, there may be some fraction of remnant SBHs formed in the aftermath of gas poor mergers, where gas torques are insufficient to prevent the high velocity recoil, launching the SBH out of the potential well of a host bulge or a host galaxy. One unique spectral signature of such systems could result from the distortion of a nuclear accretion disk and due to the velocity shift of the portion of the disk that is gravitationally bound to the SBH. On the basis

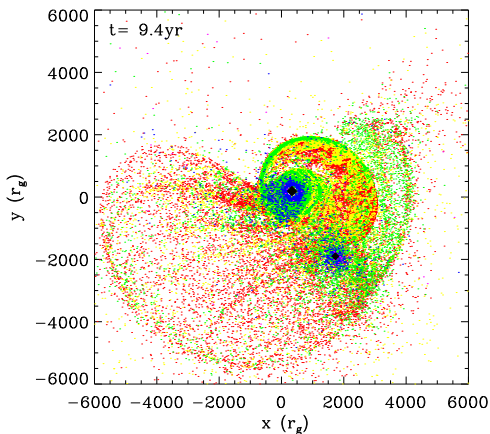


Figure 3: Snapshot from a simulation showing a SBHB and gas projected onto the plane of the binary orbit in the co-rotating model at 9.4 yr after the beginning of the simulation. The rotation of the binary and the disk is counter-clockwise. The temperatures of gas particles are marked with color: red  $T < 10^4$  K; yellow  $10^4 \text{ K} < T < 10^6$  K; green  $10^6 \text{ K} < T < 10^8$  K; and blue  $10^8 \text{ K} < T < 10^{10}$  K. The higher temperature particles are plotted over the lower temperature ones, with the result that some information is hidden. Figure 4 illustrates this effect and can also be used as a color bar. Figure adapted from Bogdanović et al. (2008).

of this signature, Komossa et al. (2008) reported a discovery of the first recoiling SBH candidate, J0927, followed by J1050, reported by Shields et al. (2009b), (see §1.1).

Therefore, the emission-line Doppler shift has so far been a key signature, sought after in screenings for both the SBHB and recoiling SBH candidates. In order to utilize it to its full potential, and in anticipation of even richer data sets in the future, expanded towards higher redshifts and lower-luminosity AGN, it is necessary to gain understanding of the remainder of associated emission signatures in other wavelength bands. An opportunity to study observational signatures in parallel with observations is offered by hydrodynamics simulations of SBHBs interacting with gas. In the following section we describe some of the advancements and challenges associated with this approach in general and then present selected results from our work.

### 3. Simulations of SBHBs and gas

Over the past several years simulations of merging galaxies have significantly contributed to our understanding of the formation and evolution of black hole pairs (as discussed at the beginning of §2). However, simulations that would span without gaps the entire dynamical range from a galactic merger to binary coalescence are still computationally prohibitively expensive. In order to reduce this problem into one that is numerically tractable it is currently necessary to make simplifications in the initial conditions and the treatment of the thermodynamics of the gas. These choices include black hole pairs initialized in steady-state galactic and nuclear accretion disks, while in reality they are most likely to be perturbed and possibly heavily irradiated by one or two AGNs. The treatment of gas thermodynamics in such disks may involve a parametric

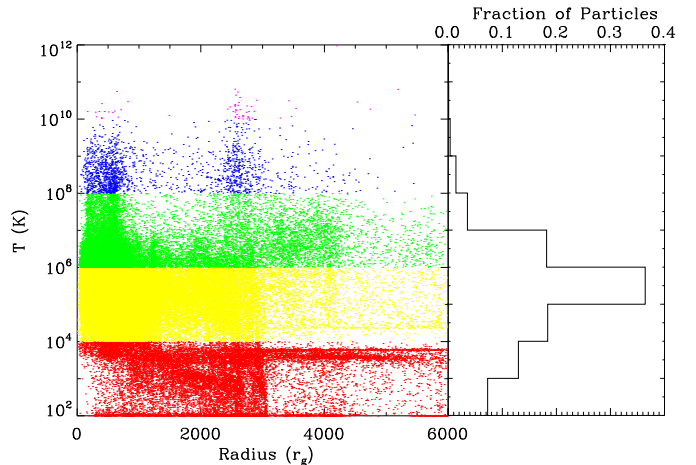


Figure 4: *Left*: Temperatures of gas particles as a function of radius at 9.4 years in the co-rotating model simulation. This figure shows the extent of temperature stratification in the disk. Different colors that mark each temperature band are equivalent to those in the previous figure. This figure corresponds to the morphology of the disk shown in Figure 3. *Right*: Histogram showing the temperature distribution of particles. Figure adapted from Bogdanović et al. (2008).

prescription in the form of a fixed equation of state or a cooling law parametrized in terms of the dynamical time scale of a system ( $\beta$ -model). These simplifying assumptions result in uncertainties in the evolution of the SBHBs with the smallest (sub-parsec) orbital separations; such binaries are also the most interesting because of their proximity to gravitational wave regime and coalescence. Further improvements in the treatment of gas thermodynamics can be made thus reducing one of the two dominant sources of uncertainty (the other one being the initial conditions). This can be achieved by adopting a more physically motivated form for gas cooling and also gas heating by introducing the sources of ionization associated with the accreting SBHBs.

Given the challenges associated with the detection of SBHBs and recoiling SBHBs, predictions of observational signatures based on existing hydrodynamical simulations would be very valuable. This is currently not attainable because hydrodynamical models do not include radiative transfer prescriptions that allow such predictions to be made (the exception are the accretion rate curves, which are also subject to the uncertainties described in the previous paragraph). Indeed, a complete treatment of radiative transfer within a hydrodynamical simulation of SBHBs and non-zero metallicity gas is currently not feasible. Nevertheless, a significant step toward this goal can be made with the help of photoionization codes that include full radiative transfer treatment of gas composed of multiple atomic species and can make a variety of predictions in the form of characteristic emission lines and continua, associated optical depths, and a plethora of other information. Photoionization codes can be used to characterize radiative transfer within every individual parcel of gas in a simulation, given the physical properties at the location of a parcel (number of ionizing photons, temperature, and density of the gas). Because the range of physical proper-

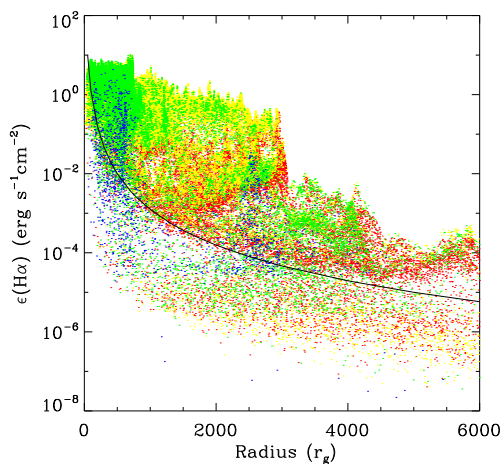


Figure 5:  $H\alpha$  emissivity of the gas as a function of radius, at 9.4 years for a co-rotating model with solar metallicity gas. The emissivity of each gas cell plotted in the figure is weighted by the density of the gas at that position, so that comparison with the parametric emissivity model (plotted as a solid line with arbitrary normalization) can be made. The color legend is the same as in previous two figures. Figure adapted from Bogdanović et al. (2008).

ties in a simulation can be predicted with some certainty (based on the properties of nuclear regions in galaxies hosting AGNs or from test simulations), the response of the gas to photoionization *precomputed* and stored in a database. Such a database can be used for reference during simulations (for an example of this approach see Bogdanović et al., 2008), or in some cases in the post-processing of simulation data (Bogdanović et al., 2004), in order to calculate observational signatures. The main effort associated with this approach is the calculation of well behaved heating, cooling, and emissivity maps (within the limits of the specific photoionization code). The computational cost associated with the addition of the photoionization data grid to the hydrodynamical code is modest, as the majority of the additional operations are interpolations between the grid points. While any such method must acknowledge that detailed modeling of emission line and other spectral properties is currently still out of reach, it still offers the best means of examining the most *characteristic* signatures of sub-parsec SBHBs and recoiling SBHBs.

In the following section we summarize the results from such a study of observational signatures of SBHBs interacting with gas.

### 3.1. Investigations of observational signatures using multi-species radiative transfer

We implemented an approximate multi-species radiative transfer scheme in a modified version of the smoothed particle hydrodynamics (SPH) code *Gadget 1* (Springel et al., 2001) in order to study the observational signatures of sub-parsec binaries interacting with gas (Bogdanović et al., 2008). The gas is assumed to have solar metallicity and its physical properties were characterized by calculating heating, cooling, and radiative processes as an integral part of hydrodynamical simulations. Using photoionization code *Cloudy* (Ferland et al.,

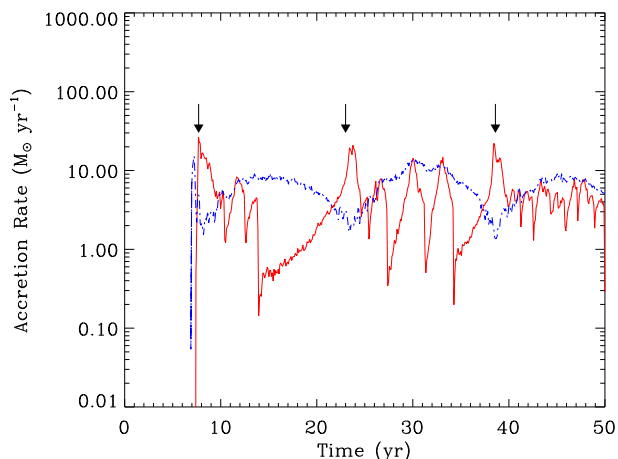


Figure 6: Effective accretion rate on the primary (*solid, red line*) and secondary (*dashed, blue line*) black hole calculated from co-rotating model. Note that in this figure only we show data from a lower resolution test simulation (20k particles) which ran over a longer period of time ( $\sim 50$  yr) than the baseline 100k simulation ( $\sim 35$  yr) but is in all other aspects equivalent to it. The accretion rates can be translated into UV/X-ray luminosity by assuming  $1 M_{\odot} \text{ yr}^{-1} \approx 10^{43} \text{ erg s}^{-1}$  in the UV/X-ray band. The arrows mark the times of the pericentric passages of the binary. Figure adapted from Bogdanović et al. (2008).

1998), we constructed a grid of photoionization maps for a range of parameters, determined from preliminary simulations without cooling. The maps are calculated in the parameter space of *density* and *temperature* of the gas and *intensity* of the ionizing radiation. The range of parameter values for which the maps were computed is as follows:  $10^9 \text{ cm}^{-3} < n < 10^{19} \text{ cm}^{-3}$ ,  $2000 \text{ K} < T < 10^8 \text{ K}$ , and  $0 \text{ erg cm}^{-2} \text{ s}^{-1} < J < 10^{17} \text{ erg cm}^{-2} \text{ s}^{-1}$ . Gas at higher temperatures than  $10^8 \text{ K}$  is also found in our simulations; in such cases we calculate heating and cooling rates and other properties of interest by linearly extrapolating the grid values. In the SPH simulations we set the lower threshold for the gas temperature to 100 K and assign no upper threshold. Based on these results we calculated the accretion-powered continuum and  $H\alpha$  light curves, as well as the  $H\alpha$  emission line profiles emerging from the inner parts of a gas disk in the presence of a binary, on a scale of  $< 0.1$  pc. We selected the Balmer series  $H\alpha$  line ( $\lambda_{\text{rest}} = 6563 \text{ \AA}$ ) because it reflects the kinematics in the broad line region of AGN (e.g., Sulentic et al., 2000). Hence, by mapping the kinematics in the region of sub-parsec size, broad  $H\alpha$  line can in principle provide important information about SBHBs interacting with gas<sup>2</sup>. Moreover,  $H\alpha$  is the most prominent broad line in the optical spectrum, least contaminated by neighboring narrow emission lines. The  $H\alpha$  line in accretion-powered sources is thought to be powered by illumination of a disk by an AGN and the radiative transfer associated with it is relatively well understood (Collin-Souffrin & Dumont, 1989). That said, the method can be extended to include other transitions of inter-

<sup>2</sup>We do not model the narrow component of  $H\alpha$  line which is thought to originate at larger distances.



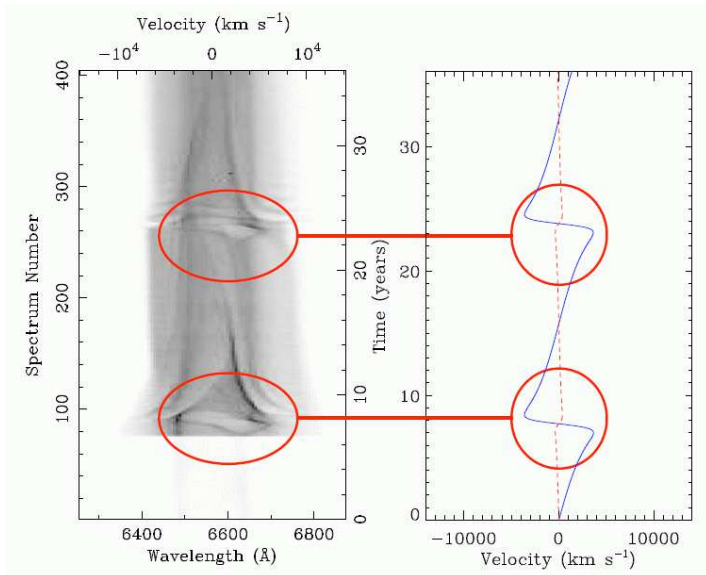


Figure 7: Trailed spectrogram (left) and black hole projected velocity curves (right) plotted for the co-rotating model. Trailed spectrogram is a logarithmic gray scale map of the  $H\alpha$  intensity against wavelength and observed velocity. Darker shades mark higher intensity. Notice the low relative intensity of the profiles before the start of accretion. The velocity curve panel shows the orbital velocities of the primary (*dashed, red line*) and secondary (*solid, blue line*) black holes projected along the line of sight to the observer. The velocity curves are skewed because of the non-zero eccentricity of the orbit. Characteristic features associated with the pericentric passages of the binary in years 8 and 23 are marked on both figures. Figure adapted from Bogdanović et al. (2008).

est, given that calculation of the photoionization data grid with *Cloudy* includes a wide range of atomic species from hydrogen to zinc.

### 3.1.1. Physical properties of the gas:

In the remainder of this section we focus on selected results from the simulation of the binary co-rotating with the gas disk and refer the reader to the original publication for discussion of the counter-rotating case. The simulation follows the evolution of a SBHB over 35 years in total and comprises  $10^5$  SPH gas particles (100k hereafter). The black hole mass ratio is 10:1, with the primary having a nominal mass of  $M_1 = 10^8 M_\odot$ . The secondary SBH is on an eccentric orbit around the primary with  $e = 0.7$ , and the initial orbital period of the binary is close to 16 years. The gas disk is initially associated with the primary black hole only and its mass and outer radius are initially  $10^4 M_\odot$  and  $2 \times 10^3 r_g$  ( $r_g \equiv GM_1/c^2$ ). The median value of the initial disk density is  $\sim 10^{13} \text{ cm}^{-3}$ . The geometry of the system and the temperature of the gas are illustrated in Figure 3 at  $t = 9.4 \text{ yr}$  after the beginning of the simulation. The primary SBH is initially located at  $(x, y, z) = (0, 0, 0)$  and exhibits modest orbital motion during the simulation.

The gas in the simulation is heated by shocks that arise from interactions with the secondary SBH and by radiation once the accretion onto the black holes begins. As a result, a portion of the gas is blown out of the plane of the disk and forms a hot halo that envelops the disk. The gas quickly departs from the uniform initial temperature of 2000 K and assumes a wide

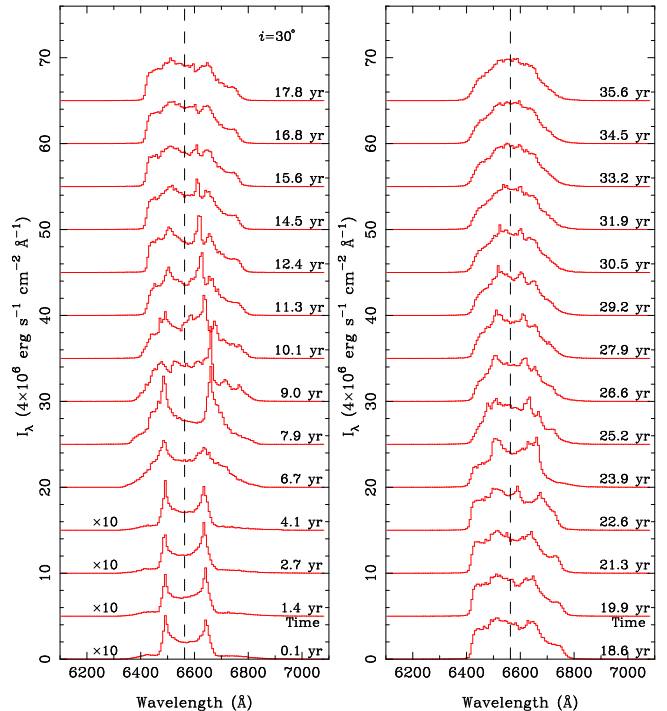


Figure 8: Sequence of  $H\alpha$  emission-line profiles selected from a model where the disk is co-rotating with respect to the orbit of the SBHB. The intrinsic intensity of profiles is plotted against wavelength. The first 4 profiles in the sequence are multiplied by a factor of 10, so that they can be represented on the same intensity scale with the other profiles. The corresponding time from the beginning of the simulation is given next to each profile. The observer is located at infinity, in the positive  $xz$ -plane at an angle of  $i = 30^\circ$  with respect to the axis of the binary orbit. Figure adapted from Bogdanović et al. (2008).

range of temperatures, as shown in Figure 4. Figure 4 further illustrates that multiple temperature components can be present at a single radius and shows the temperature distribution of the SPH particles. The hot component of the gas spends a significant amount of time in the temperature range  $10^4 - 10^8 \text{ K}$  and in this regime radiative cooling is dominated by free-free emission and recombination. The highest value of the gas temperature in the simulation,  $T \sim 10^{12} \text{ K}$ , is reached after the shock is formed by the secondary. On a time scale of months, the temperature of the gas falls below  $10^{10} \text{ K}$  due to the combined effects of radiative cooling and adiabatic expansion. On the other hand, the cold component of the gas, confined to the higher density spiral arm has a temperature in the range  $10^3 - 10^4 \text{ K}$ , close to the initial value, and cools largely through recombination radiation. At the end of the simulation the gas density in the disk is in the range  $10^8 - 10^{14} \text{ cm}^{-3}$ . The median density in the tenuous, photoionized halo is  $10^7 - 10^8 \text{ cm}^{-3}$  and the minimum density can be as low as  $10^5 \text{ cm}^{-3}$ .

The interaction of the binary with the gas also affects the emissivity of the gas and consequently its emission signatures. The most important consideration in the calculation of the emitted  $H\alpha$  light is the efficiency with which the gas reprocesses the incident ionizing radiation and re-emits it in the form of  $H\alpha$  photons. This efficiency is commonly characterized by the surface emissivity of the gas. The emissivity of the photoionized

gas depends on numerous physical parameters. Locally, it depends on the physical properties of the gas. Globally, its spatial distribution depends on the structure of the accretion disk. We assess the  $H\alpha$  emissivity of every gas particle in the simulation using photoionization data grids precomputed with *Cloudy*. In Figure 5 we compare the emissivity determined from our photoionization calculations with the parametric model used for AGNs in which the emissivity is described as a function of radius,  $\epsilon \sim \xi^{-q}$  with  $q \approx 3$  (Collin-Souffrin & Dumont, 1989). We find a qualitative agreement between the two albeit, with a significant amount of scatter. This is not surprising given the variations in surface density of the perturbed gas disk in our binary model.

### 3.1.2. Characteristic observational signatures:

We further find that X-ray outbursts (powered by accretion onto the two AGN and shocks) should occur during pericentric passages of a coplanar binary as long as the nuclear region is not devoid of gas. During pericentric passages the binary accretion rate reaches  $\sim 30 M_{\odot} \text{ yr}^{-1}$  (Figure 6), comparable to the Eddington rate for this system, while during the remainder of the orbital period the total accretion rate averages at the level of few  $M_{\odot} \text{ yr}^{-1}$ . This implies luminosity of  $L_E \approx 1.5 \times 10^{46} M_8 \text{ erg s}^{-1}$  during outbursts and an order of magnitude lower luminosity on average. Despite the 10:1 mass ratio the two SBHs exhibit comparable accretion rates and at some times the accretion rate onto the secondary exceeds that of the primary SBH. This inversion happens the lower mass object has a smaller relative velocity with respect to the gas than the primary and can result in a higher relative luminosity of a lower mass object (Artymowicz & Lubow, 1996; Gould & Rix, 2000; Hayasaki et al., 2007). During this same period the integrated (bolometric) luminosity of the disk is at a mean level of  $\sim 10^{45} \text{ erg s}^{-1}$ , and thus, comparable to that of the photoionization sources.

At the mean level of accretion inferred from the simulation, the gaseous disk should be depleted after only  $10^3 - 10^4 \text{ yr}$ . In order for the outburst activity to last over longer time scales, the reservoir of gas in the nuclear region needs to be continually replenished. It is also plausible, however, that repeated collisions of the secondary black hole with the disk will completely disrupt it and turn it into a spherical halo of hot gas. In such a case, the accretion rate would be relatively smooth and uniform, and no outburst would be evident. A calculation following the X-ray light curve variability over a large number of orbits is necessary in order to confirm that the periodicity is a long-lived signature of the binary. Although currently not possible with the SPH method used here, simulations of the long term evolution of the binary together with hydrodynamics and radiative transfer may be achieved in the future.

In addition to the recurrent outbursts in the X-ray light curve the signature of a binary is potentially discernible in the  $H\alpha$  light, and more specifically,  $H\alpha$  emission line profiles. After the start of accretion, the  $H\alpha$  luminosity reaches  $10^{39} - 10^{40} \text{ erg s}^{-1}$ , observable out to the distance of the Virgo Cluster (16 Mpc) and possibly up to the distance of the Coma cluster (100 Mpc). The changes in the profile sequence are easiest to discern in the

trailed spectrogram (shown in the left panel of Figure 7) which represents a 2D map of the  $H\alpha$  intensity against observed velocity (or wavelength). The Doppler boosting of the blue side of the line and gravitational redshift of the red wing are noticeable during the pericentric passages of the binary and, in principle, can serve as indicators of the orbital period. The width of the  $H\alpha$  profile increases after the pericentric passages of the system, reflecting the inflow of gas towards the primary. Also, the widening of the profile is asymmetric and slightly shifted towards the red with respect to the pre-pericentric sequence of profiles. This shift is a signature of the motion of the accretion disk which follows the primary that is receding from the observer. In Figure 7 we compare the trailed spectrogram with the velocity curves of the two binary components projected onto the line of sight to the observer and highlight the instances of pericentric passages. The variations in the profile intensities correspond to the features in the velocity curve of the secondary in years 8 and 23, when it is moving towards the observer with the highest projected velocity (i.e., the binary is in quadrature). Hence, we find the signatures of the velocity curves of both black holes in the emission line profiles: if such features could be discerned in the observed  $H\alpha$  emission-line profiles, they would signal the presence of a binary and potentially allow for determination of its mass ratio.

The sequence of profiles shown in Figure 8 can be obtained if the trailed spectrogram is sampled at selected times. Initially, from the unperturbed disk we observe double-peaked emission-line profiles but they gradually depart from this shape as the perturbation propagates through the gaseous disk. Our calculated profiles account only for the *broad component* of the  $H\alpha$  line; the narrow component is not taken into account. The narrow component of  $H\alpha$  is present in the observed (real) profiles and is thought to originate in gas outside of the nuclear region. Its presence adds a level of complexity to the analysis and modeling of the observed  $H\alpha$  emission-line profiles, as the narrow component of the line needs to be removed before the kinematics and geometry of the gas in the nuclear region can be assessed from the broad component of the profile.<sup>3</sup>

The irregular and variable profiles in Figure 8 are not unlike those seen in a small percentage of AGN and in SBHB candidates found in SDSS. In practice however, going from the detection of a binary candidate to a positive identification of a SBHB based on only a few epochs of observations of irregular broad Balmer lines is quite a challenging task. Our study indicates that the variability of broad emission-line profiles may be subtle and reflected in the extended wings of the profiles. In that sense an expectation that the orbital motion of the binary can be inferred from the velocity shift of the profile peaks may be simplistic and it may yield unreliable results.

<sup>3</sup>For a more detailed discussion of phenomena that may affect the shape of the  $H\alpha$  emission line profiles as well as the effect of approximations made in the calculation see Bogdanović et al. (2008).

## 4. Conclusions

Understanding the population of SBHBs near coalescence in the local universe can provide insight into the population at high redshift where theoretical models suggest most mergers take place (Sesana et al., 2007b). In practice however, the search for close binaries and their post-coalescence counterparts based on their EM signatures has proven to be a difficult task. There is only a handful of observed bound SBHB candidates and no confirmed cases at all. Thus, our understanding of the accretion physics and associated observational signatures is poor. Given the challenges associated with detection of SBHBs and recoiling SBHBs it would be valuable to make predictions of related observational signatures using hydrodynamical simulations. While some steps have been taken in that direction, more development is needed in the future in order to calculate multi-band observational signatures of these objects.

Our pilot study implies that the period and perhaps the mass ratio of the binary can be measured from well-sampled, long-term X-ray and optical light curves and  $H\alpha$  profile sequences that have been followed for at least a few revolutions of the binary. In order to achieve an efficient SBHB search and avoid time-consuming observational followups of non-SBHB candidates (false positives) it is important to utilize all available complementary signatures that may help to break this degeneracy. Given the location of selected SBHB and recoiling SBHB candidates on the sky, the best prospect for detection is with radio interferometers, if both black holes have associated radio sources. More immediate tests of existence and coalescence of binaries may be possible in the future in synergy with GW observations, once the *Laser Interferometer Space Antenna* become operational.

We would like to thank the anonymous referee for insightful comments and suggestions. TB thanks the UMCP-Astronomy Center for Theory and Computation Prize Fellowship program for support.

## References

Armitage, P. J. & Natarajan, P. 2002, *Astrophys. J. Lett.*, 567, L9  
Artymowicz, P., & Lubow, S. H. 1996, *Astrophys. J. Lett.*, 467, L77  
Baker, J. G., Boggs, W. D., Centrella, J., Kelly, B. J., McWilliams, S. T., Miller, M. C., & van Meter, J. R. 2007, *Astrophys. J.*, 668, 1140  
Baker, J. G., Centrella, J., Choi, D.-I., Koppitz, M., van Meter, J. R., & Miller, M. C. 2006, *Astrophys. J. Lett.*, 653, L93  
Begelman, M. C., Blandford, R. D., & Rees, M. J. 1980, *Nature*, 287, 307  
Berczik, P., Merritt, D., Spurzem, R. & Bischof, H.-P., 2006, *Astrophys. J. Lett.*, 642, 21  
Bogdanović, T., Eracleous, M., Mahadevan, S., Sigurdsson, S., & Laguna, P. 2004, *Astrophys. J.*, 610, 707  
Bogdanović, T., Reynolds, C. S., & Miller, M. C. 2007, *Astrophys. J. Lett.*, 661, L147  
Bogdanović, T., Smith, B. D., Sigurdsson, S., & Eracleous, M. 2008, *Astrophys. J. Suppl.*, 174, 455  
Bogdanović, T., Eracleous, M., & Sigurdsson, S. 2009, *Astrophys. J.*, 697, 288  
Borson, T. A., & Lauer, T. R. 2009, *Nature*, 458, 53  
Campanelli, M., Lousto, C., Zlochower, Y., & Merritt, D. 2007a, *Astrophys. J. Lett.*, 659, L5  
Campanelli, M., Lousto, C. O., Zlochower, Y., & Merritt, D. 2007b, *Physical Review Letters*, 98, 231102  
Chornock, R., et al. 2009a, *The Astronomer's Telegram*, 1955, 1  
Chornock, R., et al. 2009b, *Astrophys. J. Lett.*, submitted (arXiv:0906.0849)

Collin-Souffrin, S. & Dumont, A.M. 1989, *A&A*, 213, 29  
Colpi, M., Dotti, M., Mayer, L., & Kazantzidis, S. 2007 (arXiv:0710.5207)  
Cuadra, J., Armitage, P. J., Alexander, R. D., & Begelman, M. C. 2009, *Mon. Not. R. astr. Soc.*, 393, 1423  
Decarli, R., Reynolds, M. T., & Dotti, M. 2009a, *Mon. Not. R. astr. Soc.*, 397, 458  
Decarli, R., Dotti, M., Falomo, R., Treves, A., Colpi, M., Kotilainen, J. K., Montuori, C., & Uslenghi, M. 2009b (arXiv:0907.5414)  
Devecchi, B., Rasia, E., Dotti, M., Volonteri, M., & Colpi, M. 2009, *Mon. Not. R. astr. Soc.*, 394, 633  
Dotti, M., Colpi, M., & Haardt, F. 2006, *Mon. Not. R. astr. Soc.*, 367, 103  
Dotti, M., Colpi, M., Haardt, F., & Mayer, L. 2007, *Mon. Not. R. astr. Soc.*, 379, 956  
Dotti, M., Montuori, C., Decarli, R., Volonteri, M., Colpi, M., & Haardt, F. 2009, *Mon. Not. R. astr. Soc.*, L284 (arXiv:0809.3446)  
Escala, A., Larson, R. B., Coppi, P. S., & Mardones, D. 2004, *Astrophys. J.*, 607, 765  
Escala, A., Larson, R. B., Coppi, P. S., & Mardones, D. 2005, *Astrophys. J.*, 630, 152  
Ferrarese, L., & Ford, H. 2005, *Space Science Reviews*, 116, 523  
Ferland, G. J., Korista, K. T., Verner, D. A., Ferguson, J. W., Kingdon, J. B., & Verner, E. M. 1998, *Publ. astr. Soc. Pacif.*, 110, 761  
Gaskell, C. M. 2009, arXiv:0903.4447  
González, J. A., Spherhake, U., Brüggemann, B., Hannam, M., & Husa, S. 2007, *Physical Review Letters*, 98, 091101  
Gould, A. & Rix, H. 2000, *Astrophys. J. Lett.*, 532, L29  
Hayasaki, K., Mineshige, S., & Sudou, H. 2007, *Publ. astr. Soc. Japan*, 59, 427  
Hayasaki, K. 2009, *Publ. astr. Soc. Japan*, 61, 65  
Haehnelt, M. G. & Kauffmann, G. 2002, *Mon. Not. R. astr. Soc.*, 336, L61  
Heckman, T. M., Krolik, J. H., Moran, S. M., Schnittman, J., & Gezari, S. 2009, *Astrophys. J.*, 695, 363  
Herrmann, F., Hinder, I., Shoemaker, D., & Laguna, P. 2007a, *Classical and Quantum Gravity*, 24, 33  
Herrmann, F., Hinder, I., Shoemaker, D., Laguna, P., & Matzner, R. A. 2007b, *Astrophys. J.*, 661, 430  
Ivanov, P. B., Papaloizou, J. C. B., & Polnarev, A. G. 1999, *Mon. Not. R. astr. Soc.*, 307, 79  
Kazantzidis, S., et al. 2005, *Astrophys. J. Lett.*, 623, L67  
Kocsis, B., & Loeb, A. 2008, *Physical Review Letters*, 101, 041101  
Komossa, S., Zhou, H., & Lu, H. 2008, *Astrophys. J. Lett.*, 678, L81  
Komossa, S., Burwitz, V., Hasinger, G., Predehl, P., Kaastra, J. S., & Ikebe, Y. 2003, *Astrophys. J. Lett.*, 582, L15  
Kormendy, J. & Richstone, D. 1995, *Ann. Rev. Astr. Astrophys.*, 33, 581  
Lauer, T. R., & Borson, T. A. 2009, *Astrophys. J.*, accepted (arXiv:0906.0020)  
Lippai, Z., Frei, Z., & Haiman, Z. 2008, *Astrophys. J. Lett.*, 676, L5  
Loeb, A. 2007, *Physical Review Letters*, 99, 041103  
Maness, H. L., Taylor, G. B., Zavala, R. T., Peck, A. B., & Pollack, L. K. 2004, *Astrophys. J.*, 602, 123  
Mayer, L., Kazantzidis, S., Madau, P., Colpi, M., Quinn, T., & Wadsley, J. 2007, *Science*, 316, 1874  
Merritt, D., Milosavljević, M., Favata, M., Hughes, S. A., & Holz, D. E. 2004, *Astrophys. J. Lett.*, 607, L9  
Milosavljević, M. & Phinney, E.S., 2005, *Astrophys. J. Lett.*, 622, 93  
Mohayaee, R., Colin, J., & Silk, J. 2008, *Astrophys. J. Lett.*, 674, L21  
O'Neill, S. M., Miller, M. C., Bogdanović, T., Reynolds, C. S., & Schnittman, J. D. 2009, *Astrophys. J.*, 700, 859  
Perets, H. B., Hopman, C., & Alexander, T. 2007, *Astrophys. J.*, 656, 709  
Peterson, B. M. & Wandel, A. 2000, *Astrophys. J. Lett.*, 540, L13  
Richstone, D., et al. 1998, *Nature*, 395, A14  
Rodriguez, C. et al. 2006, *Astrophys. J.*, 646, 49  
Sesana, A., Haardt, F., & Madau, P. 2007a, *Astrophys. J.*, 660, 546  
Sesana, A., Volonteri, M., & Haardt, F. 2007b, *Mon. Not. R. astr. Soc.*, 377, 1711  
Schnittman, J. D., & Krolik, J. H. 2008, *Astrophys. J.*, 684, 835  
Shields, G. A., & Bonning, E. W. 2008, *Astrophys. J.*, 682, 758  
Shields, G. A., Bonning, E. W., & Salviander, S. 2009a, *Astrophys. J.*, 696, 1367  
Shields, G. A., et al. 2009b, *Astrophys. J. Lett.*, submitted (arXiv:0907.3470)  
Springel, V., Yoshida, N., & White, S. D. M. 2001, *New Astronomy*, 6, 79  
Sulentic, J. W., Marziani, P., & Dultzin-Hacyan, D. 2000, *Ann. Rev. Astr. Astrophys.*, 38, 521



Valtonen, M. J., et al. 2008, *Nature*, 452, 851  
Volonteri, M. Haardt, F., & Madau, P. 2003, *Astrophys. J.*, 582, 559  
Volonteri, M., Miller, J. M., & Dotti, M. 2009, arXiv:0903.3947  
Wrobel, J. M., & Laor, A. 2009, *Astrophys. J. Lett.*, 699, L22